Friction

Research Article

Understanding and misleading texture perception by rendering vibrational tactile stimuli

Livia Felicetti[1,2,✉], Eric Chatelet[2], Francesco Massi[1]

Cite this article: Felicetti L, Chatelet E, Massi F. *Friction* 2026, **14**(4): 9441195. https://doi.org/10.26599/FRICT.2025.9441195

ABSTRACT: Among the mechanical stimuli that arise in the tactile interaction between finger and surface during the tactile exploration, stimulating the mechanoreceptors, Friction-Induced Vibrations (FIV) play a fundamental role in discriminating the surface textures. Although it is well known that vibrational tactile stimuli strongly depend on the characteristics of the explored textures, the correlation between the different FIV features (such as amplitude and spectral distribution) with the texture perception and discrimination is still an open field of research. A vibrotactile rendering device has been here used to replicate the FIV measured when exploring isotropic textures. A sensory campaign has been conducted on 10 participants to investigate their ability to discriminate real and rendered isotropic textures, while the reproduced FIV have been manipulated and altered to mislead tactile perception. By swapping the FIV amplitudes measured from real textures, it has been observed that the participants discriminate the samples consistently with the vibration amplitude. The campaign has allowed to correlate the FIV amplitude and its frequency distribution with the perceptual results of the discrimination campaigns on real and mimicked textures.

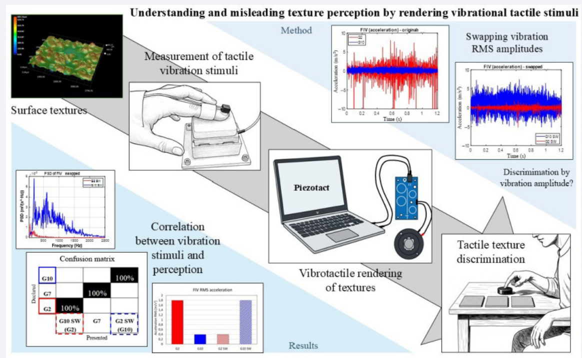

KEYWORDS: Friction-Induced Vibrations (FIV); tactile perception; tactile rendering; texture discrimination

1 Introduction

Our perception of the surrounding environment is mediated by five sensory channels, i.e., the five senses. Differently from the senses of sight, taste, smell, and hearing (relying on dedicated organs), the sense of touch relies on stimuli that come from the entire body periphery and the entire musculoskeletal system. Moreover, unlike sight and hearing, touch requires physical interaction between the skin and the object to be perceived. Touch is thus one of the most complicated and, to date, the least understood of the five senses. To date, we are able to master acoustic and sight stimuli, we well know the stimuli underlying them (acoustic and electromagnetic waves), and we are able to render them by devices of any sort, which are part of our everyday life. Contrarily, despite the great advancement of research and knowledge that is moving forward, the mechanisms behind touch are still largely obscure. Efforts to better comprehend the mechanisms underlying touch are then being carried on with a multidisciplinary approach, by a wide range of disciplines such as Medicine, Biology, Neurosciences, Psychology, Engineering, Biomechanics, etc. The possibility to master touch could have ground-breaking social and technological implications in all fields of our everyday life, reshaping the way we interact with external virtual or real environments. Touch takes its origin by the interaction between the body and the explored surface, from which static and dynamic mechanical signals are generated, such as pressure, vibrations, temperature, etc. Such signals contribute to stimulating different types of mechanoreceptors (such as Pacinian corpuscles, Ruffini endings, Meissner's corpuscles, and Merkel disks) contained in the skin [1]. Tactile stimuli, triggering the mechanoreceptors, are then encoded into electrical signals that are transmitted to the brain, to be processed and decoded. Different open lines of research aim to understand and to artificially recreate touch mechanisms, focusing on different stimuli, such as forces, friction, and vibrations [2–9]. The role of friction in encoding the surface characteristics to mediate tactile perception has been widely investigated [10–15], and tactile rendering devices based on friction coefficient feedback are numerous in literature; between the most noteworthy approaches there is the modulation of friction, that is generally achieved by electrostatic [16–22] or ultrasonic [23–26] devices, and used in Ref. [21] to relate the vibratory signal to perceptual outcomes. Vibrational feedback in touch is deeply investigated, as well as replaying vibrations recorded from exploration of real textures [22]. In Ref. [27], a

[1] Department of Mechanical and Aerospace Engineering, Sapienza University of Rome, Roma 00185, Italy. [2] INSA Lyon, CNRS, LaMCoS, UMR5259, Villeurbanne 69621, France.

✉ Corresponding author. E-mail: livia.felicetti@uniroma1.it

Received: July 24, 2025; Revised: October 1, 2025; Accepted: November 19, 2025

neural network-based model for haptic texture rendering in real time is developed, while a single-frequency texel rendering method of fine textures is presented in Refs. [28, 29]. The results presented in Ref. [22] highlighted how vibratory magnitude appeared to correlate with perceived texture roughness. On the other hand, in Ref. [30], the authors investigate how changes in the amplitude and spatial frequency of the rendered texture translated into perceptual change by a magnitude estimation task. The perceptual capacities of different rendered tactile signals are evaluated as well, according to the fine and coarse textures, in Ref. [31]. An interesting work is reported in Ref. [32], where the authors investigate the effects of two stimulation modalities, stretch and vibration, on natural touch sensation on the volar forearm. According to the duplex-theory of tactile perception [33, 34], finer textures need to be perceived through sliding contact between skin and surface, from which Friction-Induced Vibrations (FIV) are generated. Vibrotactile rendering is implemented in tactile devices [35–39], exploiting different rendering strategies to evoke tactile feeling through vibrations generated by different actuators and dynamic exciters. Devices that combine different tactile feedbacks or integrate different sensory feedbacks, such as touch, sight, and hearing, appear as well in Refs. [40–44]. This research is collocated into the line of research investigating the role of friction-induced vibrations in tactile perception and discrimination of surface textures. Many studies have shown strong correlations between induced vibrations and tactile perception, and the role that these vibrations have in encoding the topographic characteristics of textures of different types (periodic [45–47] or isotropic [48–54], fabrics [55–58], etc.). Mechanical stimuli act as an intermediary between the characteristics of the explored surface and the neuropsychological response. Contact conditions (sliding speed and direction, contact forces, etc.) [52, 59–62] and finger characteristics (fingerprint topography and depth, skin stiffness, and moisture, etc.) [10, 26, 50, 63–66] also play a role in the tactile interaction between finger and surface, resulting in specificities in the mechanical and dynamic response at the contact. Even more specifically, in the context of the investigation of the correlation between texture topographies, vibrational stimuli and perception of textures, recent studies [38, 45, 47, 49–51] have identified different key features of FIV; amplitude and frequency distribution play a prominent role in the discrimination of textures with different surface topographies: from such studies, fine periodic textures resulted to be mainly discriminated on the basis of the FIV frequency distribution [38, 45, 47], while the amplitude of the FIV drives the discrimination of isotropic textures [49–51].

The present work aims to investigate further the role of FIV in the perception and discrimination of rigid isotropic textures, exploiting, for this purpose, the possibility to mimic the textures by means of a vibrotactile device, called Piezotact [38]. This tactile rendering device allows to replicate the FIV, previously measured during the exploration of the textures, decoupling and isolating them from the other mechanical stimuli generated at the contact between finger and texture (temperature, static and quasi-static skin deformation, etc.). The Piezotact device can be used to simulate and even alter specific FIV features (e.g., their amplitude and their frequency distribution) in order to study their role in the discrimination of specific surface topographies, by simulating either real or fake textures, with desired characteristics. Discrimination campaigns have been conducted with volunteers. In rendering the textures using the Piezotact device, the amplitude of the FIV, associated with pairs of samples, has been swapped. This swap allows for evaluating whether the volunteers discriminate the textures consistently, thus corroborating the hypothesis of the main role of the amplitude of FIV in the discrimination of isotropic textures. The ability of the vibrotactile device to alter tactile stimuli may have important technological implications, such as the possibility of creating and testing new surface textures, specially designed and capable of delivering the desired tactile sensations to the user.

2 Materials and method

2.1 Overall approach

The present work is focused on one hand to confirm the key role of the FIV amplitude in the discrimination of isotropic textures [49, 50], and on the other hand to show how a tactile rendering device, such as the Piezotact [38], can be used as a tool to alter specific features of the mechanical stimuli (here the FIV) to investigate their specific role in tactile perception or to modify perceived surface properties.

In the first instance, the contact forces and FIV stimuli have been measured when actively exploring a set of isotropic surface samples, manufactured by moulding of glasspapers. The FIV have been analyzed and then simulated by the Piezotact vibrotactile device, with the underlying rendering method [38]. The surface samples, the test bench to measure the mechanical stimuli, and the details of the Piezotact device working principle are described in Sections 2.2–2.4.

Then a sensory campaign was carried on a panel of 10 volunteers, with the protocol detailed in Section 2.6, on the real textures and on the rendered textures by the Piezotact. The aim of the discrimination campaign was to investigate the role of the FIV amplitude in the discrimination of isotropic textures. In Refs. [49, 50], the hypothesis has been formulated that the tested isotropic textures are discriminated mainly on the basis of the amplitude of the FIV stimuli. To corroborate this hypothesis, modified signals are created by swapping the amplitude of the measured FIV for some pairs of sample surfaces. The signal processing to obtain the "fake" textures is detailed in Section 2.5. The Piezotact device has been used to render the signal of these "fake" textures and then to perform discrimination tests to evaluate whether the volunteers were induced to discriminate the textures consistently with the amplitude swaps. Finally, the results of the sensory campaigns have been interpreted by analyzing the FIV.

2.2 Surface samples

A set of 13 surface samples, denoted G*i* (i = 1, …, 13), and characterized by isotropic topography was manufactured and tested in this study, replicating glasspapers with grit ratings ranging from P40 to P4000 (Table 1). The surfaces are considered "isotropic" since their topographies do not present preferential orientation or substantial topographical variations with the scanning directions. Firstly, silicon (ELKEM BLUESIL RTV 3428) molds of the glasspapers were produced; then, epoxy resin (Prochima E-30) was poured into the silicon molds. Isotropic surface samples, consisting of squares of 50 mm², were thus obtained (Fig. 1). The S_a roughnesses (with an L-Filter cutoff wavelength of 2.5 mm) of the samples reported in Table 1 were measured with a digital microscope VHX-7000 Keyence on areas of 3 mm × 3 mm. Figure 1 shows the topographies of the samples.

2.3 Measurement of mechanical stimuli from texture exploration

Friction-induced vibrations (acceleration) and contact forces were

Table 1 Glasspaper grit ratings, sample denominations, and measured S_a roughness

Glasspaper	Sample name	S_a (μm)
P40	G1	71.6
P60	G2	51.2
P80	G3	29.9
P120	G4	17.2
P180	G5	15.8
P240	G6	10.0
P400	G7	6.2
P600	G8	6.5
P800	G9	5.4
P1000	G10	4.0
P2000	G11	4.3
P2400	G12	4.0
P4000	G13	4.8

measured during active tactile exploration of the isotropic samples with the experimental setup in Fig. 2. To perform the measurements, the sample was fixed with double-sided tape on a triaxial force transducer (Testwell K3D60) to monitor the contact forces exerted during the surface scanning. An accelerometer (PCB 352A24, PCB Piezotronics Inc.) was fixed with wax on the nail of the participant's index finger of their dominant hand. During the texture exploration, the participant maintained a contact force of approximately between 0.2 and 0.4 N, and a finger/surface angle of approximately 20°. A minimum of 10 repetitions of the same exploratory movement of the finger against the surface, from distal to proximal direction, were measured and then analyzed. The signals from the transducers were acquired by a SIRIUSi (DeweSoft) DAQ system at a 5 kHz sampling frequency and then postprocessed with the Matlab (Mathworks) software. With this protocol, the FIV were measured during the exploration of each isotropic surface belonging to the set described in Section 2.2 for each of the 10 participants involved in the study.

2.4 Vibrotactile rendering device to mimic FIV stimuli

The FIV stimuli, measured during the exploration of isotropic textures, were replicated by a vibrotactile rendering device [38, 49–51] (Fig. 4), in order to carry out the sensory campaigns object of this work. The Piezotact (Fig. 3) device consists of an electro-active polymer (EAP) piezoelectric actuator [67], blocked into a PLA support (produced by additive manufacturing), and its driving chain, consisting into an electronic card (Texas Instruments (TI) DRV2667EVM-CT) able to drive the actuator, and a commercial computer used to send the desired actuation analogic signal to the TI card (Fig. 3). Vibrations along the normal direction to the actuator plane were generated and can be perceived by placing the finger on the actuator surface. To replicate the FIV measured by scanning real surfaces, the signal sent as an input to the device needs to be accurately processed to obtain a correct FIV rendering of the texture vibration on the user finger. For this purpose, the rendering strategy underlying the Piezotact working principle is based on the experimental characterization of the overall transfer function (TF) of the bio-electro-mechanic system, including the device and the user's finger [38, 49, 50]. The transfer function is determined by sending a random input signal to the device, through the personal computer (PC), and measuring the acceleration on the finger (by an accelerometer on the nail), which is in contact with the actuator. The transfer function is computed as an H1 estimator. Then, the FFT spectrum of the FIV signal, measured when scanning the texture (with the protocol in Section 2.3), is processed by dividing it by the overall system's transfer function; a new time signal is then obtained by performing an Inverse FFT, which is sent as input to the Piezotact device (Fig. 4). Since the signal is re-multiplied by the transfer function of the overall system, when passing through it, a correct FIV rendering is achieved by the device. A previous study [50] showed that good discrimination results can be obtained by using an average TF, calculated as average of the participants' specific TFs, to process the FIV, rather than using the specific transfer function of each user. This solution is therefore adopted in the present study. More details of the development and validation of the Piezotact device and the underlying texture rendering strategy can be found in Refs. [38, 49–51]. The device is capable of isolating and decoupling vibrational stimuli (FIV) from other tactile stimuli, enabling an in-depth investigation into their role in perception. Sensory campaigns can be carried out by rendering the textures by the sole FIV. In this work, the device is used as well to alter specific characteristics of the FIV signals.

2.5 Signal processing for FIV amplitude swaps

The Piezotact device was here used as a research tool to appropriately manipulate the FIV signals. Fake textures were built by swapping the FIV associated with pairs of isotropic surface samples, in terms of root mean square (RMS) amplitude, with the following signal processing, illustrated through an example. Figure 5(a) shows the FIV signals (accelerations) measured during the tactile exploration of a pair of isotropic samples (G2 and G10), while Fig. 5(c) shows their respective power spectral density (PSD). In order to generate the fake textures, the FIV signals belonging to the pairs of samples were divided by the value of their own RMS amplitude, and then, multiplied by the RMS amplitude of the FIV of the other sample belonging to the pair (Fig. 5(b) shows the swapped acceleration signals and Fig. 5(d) the associated PSD). In the example, as a result of the processing, the "G2 SWAPPED" ("G2 SW" in brief) signal has the same RMS amplitude of the "G10", and the "G10 SWAPPED" has the same RMS of the "G2", as shown in Fig. 6. With this processing, each FIV signal, associated to a sample in the pair, has its own original frequency distribution, but the RMS amplitude of the other sample belonging to the pair (Fig. 5(d)). The obtained FIV, swapped in terms of RMS amplitude, are then processed to be rendered by the Piezotact device, with the procedure in Section 2.4, in order to perform the discrimination campaigns (Section 2.6).

2.6 Discrimination campaign protocol

The sensory campaign wwas carried on 10 participants (9 males and 1 female, 1 lefthander and 9 righthanders, with ages ranging between 21 and 46 years).

The campaign protocol was articulated in 3 tasks:

(1) discrimination of the real isotropic textures (task 1);

(2) discrimination of the rendered isotropic textures by the Piezotact device, by replicating the FIV measured during the exploration of the surfaces (task 2);

(3) discrimination of the rendered isotropic textures by the Piezotact device, with FIV amplitude swaps for some pairs of samples (task 3).

The campaign was carried on using 6 sets composed by triplets of samples selected from the 13 isotropic textures. The composition of the triplets is resumed in Table 2. The third column in Table 2 presents the 2 samples that have been swapped in terms of FIV RMS amplitude, for each set, when rendered by

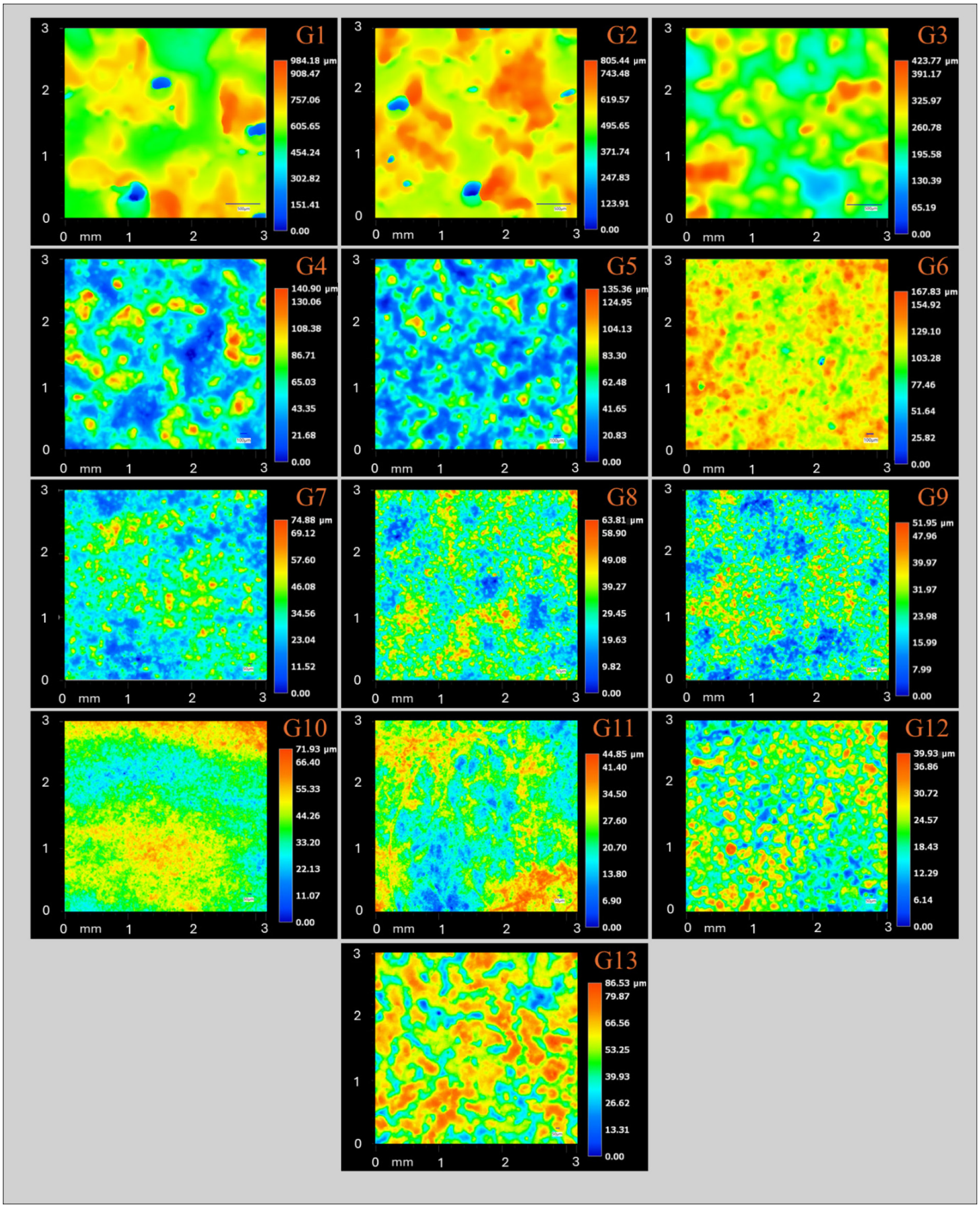

Fig. 1 Sample's topographies obtained with a WHX 7000 Keyence digital microscope.

the Piezotact in order to perform task 3. During the discrimination campaigns, the participants were equipped with scratched spectacles that allowed to identify the shape and the position of the samples but not the texture, and noise-cancelling headphones to avoid acoustic feedback by the actuator. No time limit was imposed to the participants to perform each discrimination test. The three tasks were performed with a protocol that is provided as follows.

Task 1 consisted in the discrimination of the real isotropic samples. For each set (triplet) of samples in Table 2, the participant was asked to touch and explore the textures, which were presented in a random order, with their dominant hand index finger, and to acquire familiarity with the textures. Then the volunteer was asked to sort the 3 samples from the roughest one to the smoothest one (assigning them to position A, B, C, as illustrated in Fig. 7(a)). Once the participant ranked the real sample textures (assigning them A, B, and C positions, see Fig. 7(a)), the two following tasks concerned the discrimination of the textures rendered with the Piezotact device.

Task 2 consisted in a discrimination of the rendered textures by

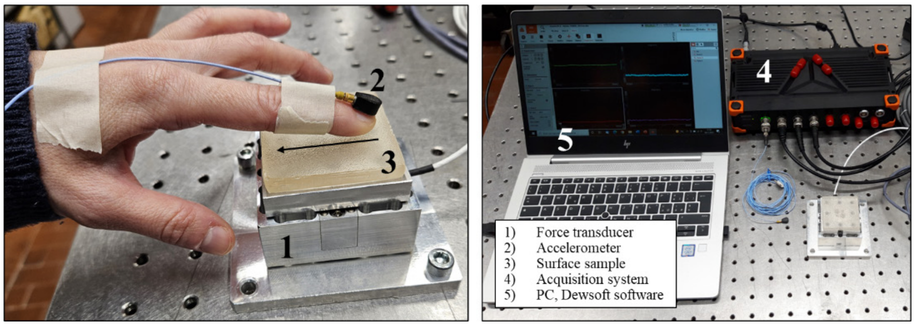

Fig. 2 Experimental setup to measure mechanical stimuli during texture exploration.

the Piezotact device (Fig. 7(b)), by replicating the corresponding FIV signals obtained by scanning of the real surface samples (protocol in Sections 2.3 and 2.4). For each set of samples in Table 2, the FIV associated to the 3 samples were presented in a random order to the participant by the Piezotact device. The participant was asked to perceive the vibrations by touching the actuator and to associate to each rendered FIV the corresponding real surface, with a forced choice matching protocol. The participant was allowed to perceive the sequence of rendered textures more than once and to touch the real samples, to compare the real and rendered textures, during the discrimination test. For each triplet of samples, 2 different random sequences of rendered textures were proposed to each participant, i.e. two discrimination tests were performed on each sample set per participant, so that each triplet was tested 20 times in the entire campaign on the 10 participants.

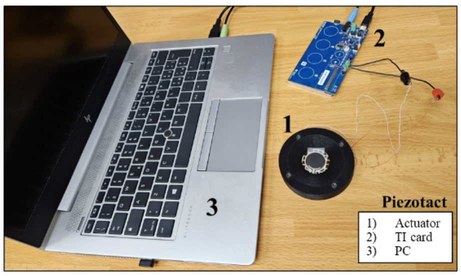

Fig. 3 Piezotact tactile rendering device.

Task 3 consisted in a discrimination of the rendered textures by the Piezotact device, with pairs of FIV swapped in terms of FIV RMS amplitude, using the signal processing presented in Section 2.5. The protocol of the discrimination campaign was identical to the protocol of task 2; i.e., for each triplet a random sequence of rendered textures by the Piezotact was proposed to the participant, who was asked to associate to each perceived vibration the corresponding real texture. The swapped pairs of samples in terms of FIV amplitude for each set are listed in column 3 of Table 2. As before, 2 different sequences per triplet have been proposed to each participant.

Tasks 2 and 3 have been randomly counterbalanced across participants and sample sets to prevent the sensory campaign from being affected by the order of the tasks.

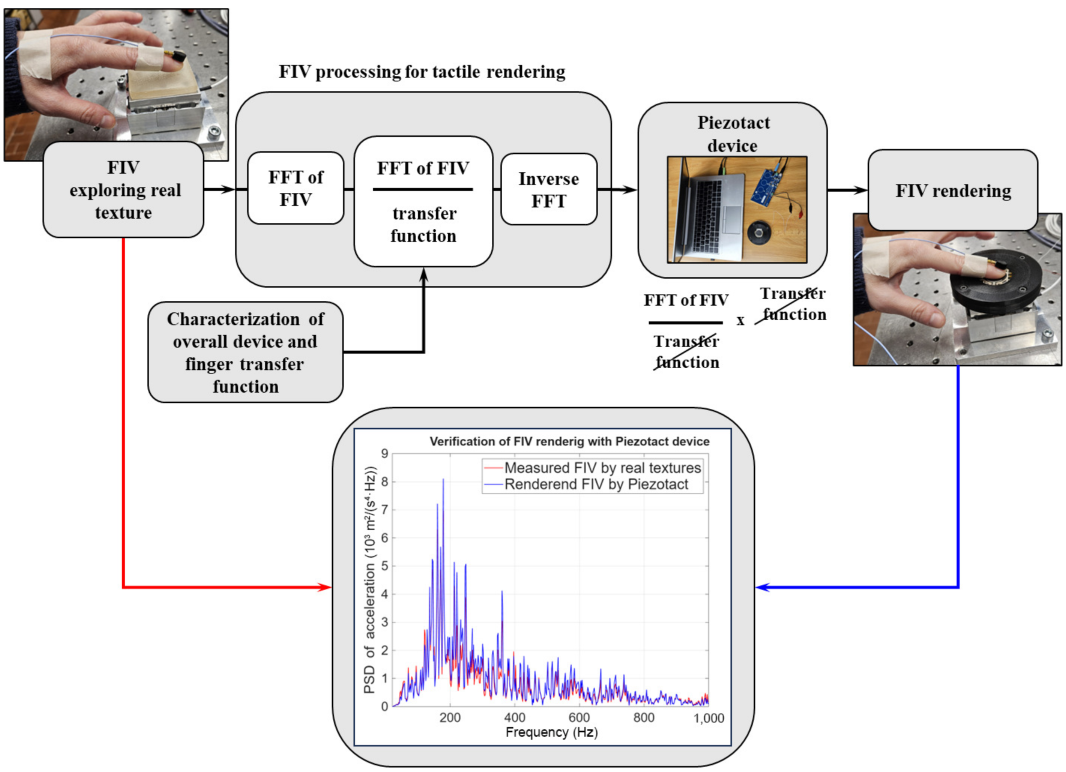

Fig. 4 Scheme of the rendering methodology based on the overall transfer function characterization, including an example of verification of FIV correct rendering by the Piezotact device, obtained by comparing the FIV spectra measured by scanning a real texture (sample G5) and the rendered FIV spectra with the device.

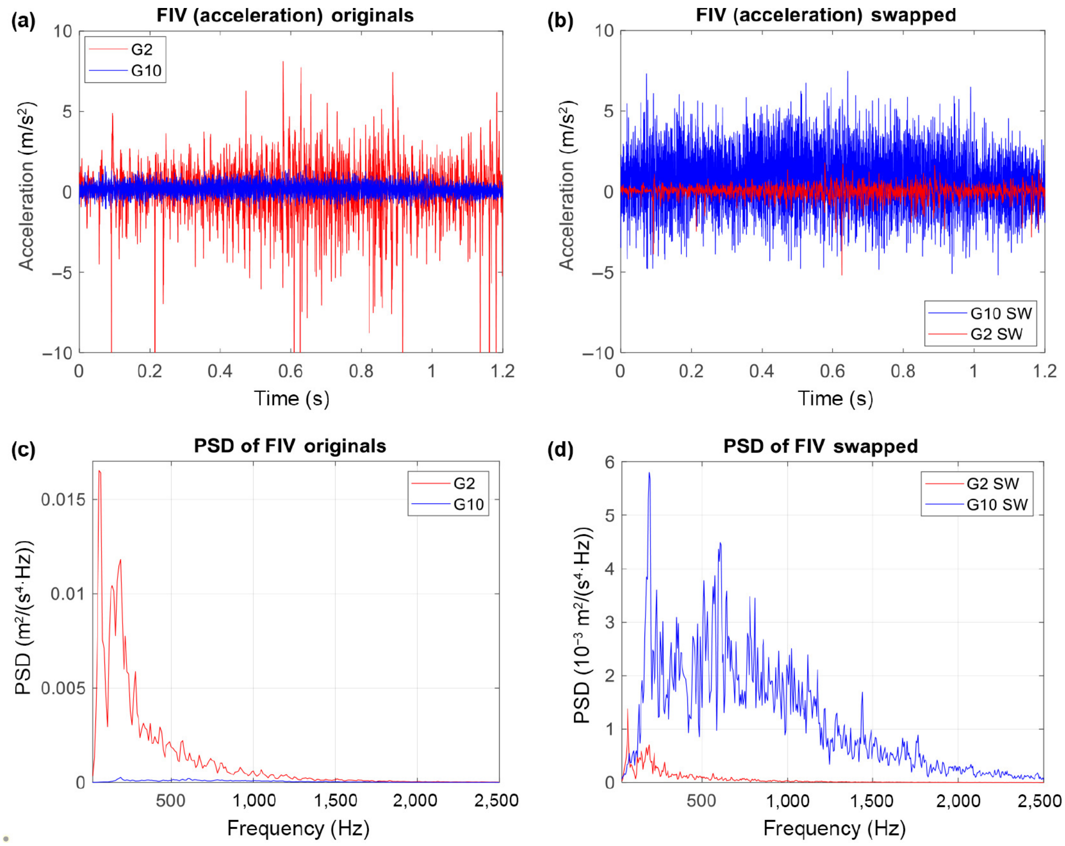

Fig. 5 Examples of swap of FIV of two surfaces based on FIV RMS amplitude: (a) FIV measured on the real surfaces; (b) FIV with amplitude swaps; (c) PSDs of FIV measured on the real surfaces; (d) PSDs of FIV with amplitude swaps.

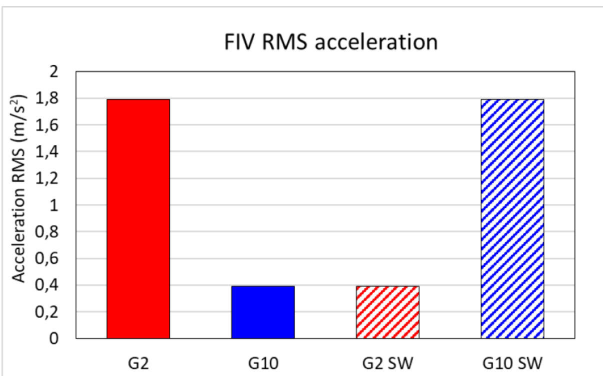

Fig. 6 Examples of values of FIV RMS amplitudes associated with the original and swapped signals for a pair of samples.

Table 2 Used sets of samples for the discrimination campaign. The thirst column shows the swapped pairs of samples, in terms of FIV amplitude, for task 3

Set	Sample	Swapped sample
Set 01	G2, G7, G10	G2, G10
Set 02	G5, G8, G11	G5, G11
Set 03	G1, G6, G13	G1, G13
Set 04	G4, G9, G12	G4, G12
Set 05	G3, G10, G11	G3, G10
Set 06	G8, G9, G13	G8, G13

Confusion matrices have been used to analyze the results of the discrimination campaigns. The sequence of the samples is arranged on the two axes (on the abscissa the presented samples to the participants and on the ordinate for the declared answers by the participants), so that the correct discriminations of the samples lie on the main diagonal of the matrix, while the discrimination errors lie outside the diagonal. The association percentages are calculated as the ratio between the number of times that an association is declared by the participants and the number of times that the sample is presented to the participants in the whole discrimination test (multiplied by 100 to obtain a percentage). As regards the campaign of discrimination of textures rendered by Piezotact with swaps of FIV amplitudes (task 3), the sequences of the samples on the axes are arranged so that samples having the same FIV RMS amplitude match on the main diagonal; in this way the associations that confirm the hypothesis that the discrimination of isotropic samples is correlated with the FIV RMS amplitude lie on the main diagonal in task 3.

The obtained data were statistically analyzed by the XLSTAT software. In task 1, i.e., the ranking of the real textures from the roughest to the least rough, a two-tailed Wilcoxon sign rank test (non-parametric test) for paired data (all tests were obtained by the same participants) was performed for each pairwise combination within each sample set (triplet), considering significant at level $\alpha = 0.05$, with $n = 10$. For tasks 2 and 3, i.e., the discrimination of simulated textures, the Wilcoxon signed rank test (with $n = 20$) was used to test whether volunteers' scores (number of correct/expected answers) were significantly above the chance level. The chance level was computed as the expected value of the correct matching of 3 samples for a forced choice test without repetitions, which is the protocol of the discrimination test in tasks 2 and 3; the possible permutations of 3 elements are $3! = 6$, and the expected value of the matching distribution (0, 1, or 3 correct answers) by chance is equal to 1. The upper-tailed Wilcoxon sign rank test for paired data was performed on each sample set, significant at level α = 0.05. The tested alternative hypothesis (Ha) was that the median of the distribution of the correct answers, provided by the participants for each sample set, exceeds the expected chance level, theoretically set at 1 (median > theoretical median = 1, n = 20).

3 Results and discussion

In this section, the results of the overall sensory campaign, performed on 10 volunteers and for all tasks, concerning the discrimination of real and rendered textures are presented. Then, the results of the sensory campaign are analyzed, interpreted, and discussed in relation to the tactile mechanical stimuli measured during the tactile exploration.

3.1 Results of sensory campaign

3.1.1 Discrimination of real textures (task 1)

The results of the discrimination campaign of the real isotropic textures (task 1), for the 10 involved participants, are presented in Fig. 8. In this task, for each set of samples, volunteers were asked to sort the samples from the roughest to the least rough. Overall, the discrimination of real textures by the participants confirms the sequence of samples in Table 1. Most of the discrepancies between the sequences chosen by the participants and the reference order of the samples (corresponding to the grit ratings in Table 1) are found in the sets 05 and 06, affecting the smoothest samples (from G8 to G13). On the contrary, in sets 01 to 04 no discrepancy is found between the participants' answers and the sequence chosen as a reference, evidenced by the percentages of 100% located on the diagonals of the confusion matrices. In set 05 most participants judged the G10 sample to be less rough than the G11 sample (70% association). In set 06, although high percentages of association (greater than 70%) are located on the main diagonal, testifying to a correspondence between the perception of the roughness of the textures by the participants and the grit ratings of the samples, some associations with lie outside the diagonal; the sequence of samples G8, G9, and G10 has not been uniformly sorted by the participants. Overall, most perceptual non-uniformities are related to the samples from G8 to G13. The Wilcoxon analysis revealed significant differences (p-value < 0.05) for each pairwise sample combination within sets 01, 02, 03, 04 (Z = −3.162, p = 0.002, and n = 10). In set 05, the sample pairs G3–G10 and G3–G11 (Z = −2.919, p = 0.004, n = 10) showed significant differences (p-value < 0.05), while the sample pair G10–G11 ($Z_{G10,G11}$= 1.265, $p_{G10,G11}$ = 0.206, and n = 10) did not show statistically significant differences (p-value > 0.05). Nevertheless, the median of the participants' answers revealed that sample G11 was judged rougher than sample G10. In set 06, the sample pairs G8–G13 ($Z_{G8,G13}$= −2.495, $p_{G8,G13}$ = 0.013, and n = 10) and G8–G9 ($Z_{G8,G9}$= −2.530, $p_{G8,G9}$ = 0.011, and n = 10) showed significant differences (p-value < 0.05), while the sample pairs G9–G13 ($Z_{G9,G13}$= −1.008, $p_{G9,G13}$ = 0.313, n = 10) were not significantly different (p-value > 0.05). The median values showed

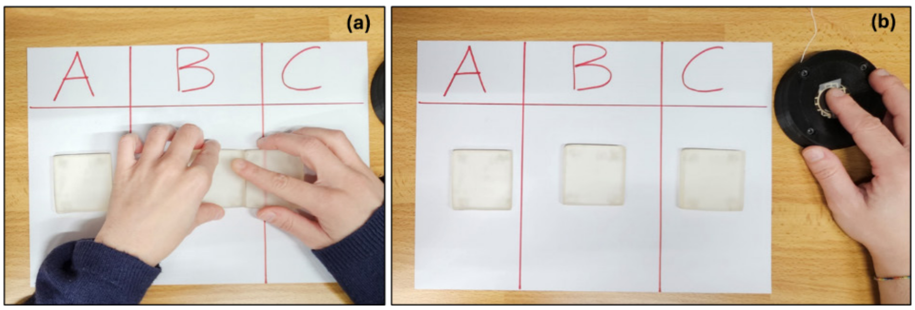

Fig. 7 Participant performing a discrimination test (a) on the real textures, i.e., task 1, and (b) on the rendered textures by the Piezotact device, i.e., task 2 or task 3.

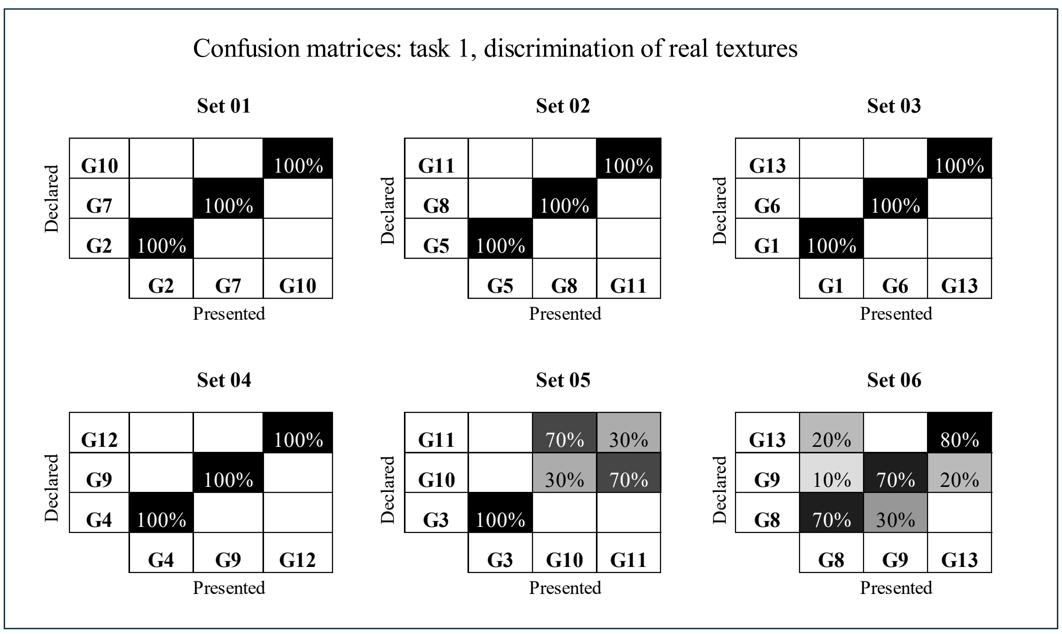

Fig. 8 Results of discrimination campaign of real textures (task 1).

a decreasing roughness judgment from sample G8 to sample G13 in set 06.

3.1.2 Discrimination of rendered textures (task 2)

The results of the discrimination campaign of the rendered textures, simulated by the Piezotact device (task 2), for the 10 involved participants, are presented in Fig. 9. In this task, participants were asked to associate the textures rendered with the device to the corresponding real samples; the textures were rendered by replicating the FIV measured during the active exploration of the samples (protocol in Section 2.6). The associations located on the main diagonals of the matrices (Fig. 9), in this task, represent the correct association between the textures rendered by FIV with the Piezotact device and the corresponding samples (previously classified by the participants) that have generated the FIV through active exploration. Overall, excellent performances are achieved by the participants in associating the rendered FIV stimuli and the corresponding real surfaces, evidenced by the high percentages located on the main diagonals of the matrices. In sets 02 and 04, some discrimination errors are found, but with low association percentages. Most of the discrimination errors with higher association percentages are found in sets 05 and 06, associated with the least rough samples (from G8 to G13), coherently with results obtained in task 1. In particular, in set 05, the G3 sample is always correctly discriminated, while the G10 and G11 samples are sometimes confused. For all the 6 sample sets, a *p*-value < 0.05 is found, indicating that the alternative hypothesis (Ha) of the Wilcoxon test must be accepted. This means that participants' responses were significantly above the chance level for all sample sets.

3.1.3 Discrimination of rendered textures with FIV amplitude swaps (task 3)

For the 10 involved participants, the results of the discrimination campaign of the rendered isotropic textures simulated introducing the FIV RMS amplitude swaps (Table 2) are presented in Fig. 10. In this task, textures were rendered by swapping FIV in terms of RMS amplitude for the specific pairs of samples. Let us keep in mind that in the confusion matrices, shown in Fig. 10, the samples are arranged on the axes so that the rendered textures having the same FIV RMS amplitude match on the principal diagonal. Overall, high percentages of association are localized, for almost all sets, on the main diagonal of the confusion matrices, confirming the hypothesis that, by swapping the amplitudes of the induced vibrations, the volunteers are misled and induced to discriminate such rendered textures consistently with the amplitude swaps. In Fig. 10, it is possible to observe that the overall trend of texture discrimination in task 3 (Fig. 10) for sets 05 and 06 agrees with the one found in task 2 (Fig. 9). In fact, in set 05, most of the unexpected associations concern samples G11 and G3 SW (having the same RMS amplitude of G10). This agrees with the confusions between G10 and G11 in task 2 (Fig. 9). In set 06 several discriminations errors occurred in task 3 (Fig. 10), even if the percentages of expected associations on the main diagonal were still high, in agreement with the discrimination in task 2 (Fig. 9). This is also in agreement with the results of task 1 on the real textures discriminations (Fig. 8), where it was found that samples from G8 to G13 were difficult to discriminate. As in task 2, also in task 3 some discrimination errors occurred in set 02 and in set 04. In set 04, some errors occurred in task 3 between samples G9 and G4 SW (having the same RMS amplitude as G12). This reflects the confusion that occurred between samples G9 and G12 in task 2 (Fig. 9), confirming the matching between the FIV RMS amplitude and the texture discrimination. It can be observed that, overall, better discrimination performance is achieved in task 2, where the textures are rendered by FIV by conserving the original amplitude and frequency distribution of the FIV measured when exploring the samples, than in task 3, where the rendered FIV have their original frequency distributions but altered amplitudes. This may suggest that, although amplitude turns out to be the key parameter for the discrimination of isotropic textures, a role may also be played by frequency distribution; it is always necessary to keep in mind that all the parameters associated with mechanical stimuli contribute to tactile perception, although it is possible to identify, in some cases, one driving parameter, that has a greater influence on perception and discrimination than others. Overall, excellent agreement is found in the results of the three discrimination tasks

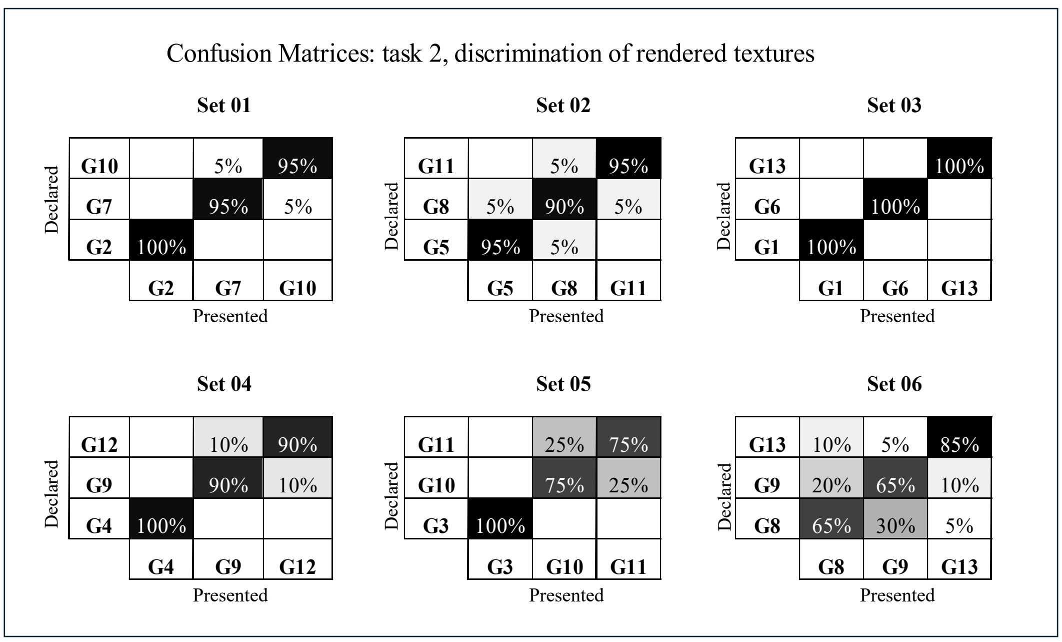

Fig. 9 Results of discrimination campaign of rendered textures with the Piezotact device (task 2).

on real and rendered (without and with amplitude swaps) textures, since the most frequently occurring errors involve the same samples and the same sets, set 05 and set 06, in all the three tasks. As found in task 2, the Wilcoxon test revealed that the sample matching provided by the participants was above the chance level for each tested sample set. In the following section, the results of the overall sensory campaign are interpreted by the analysis of the corresponding FIV stimuli.

3.2 Interpretation of sensory campaigns by FIV analysis

For each volunteer, the FIV for the 13 isotropic samples were measured by active touch using the protocol in Section 2.3. For each surface sample, the FIV measured for 10 active strokes of the finger on the surface were analyzed for each volunteer, and an average RMS FIV amplitude between the 10 analyzed strokes was computed. Then, for each sample texture, an average FIV RMS amplitude among the 10 volunteers was computed; the FIV RMS values are shown in Fig. 11 with their standard deviations. Samples from G1 to G7 have very different FIV RMS amplitudes, with a well-defined decreasing trend as the texture roughness decreases. These surfaces were always correctly discriminated by the participants in the discrimination task of the real textures (Fig. 8) for all the tested sets; i.e., the roughness judgement was in agreement with both the effective roughness of the samples (Table 1) and the amplitude of the FIV (Fig. 11). For the same textures (from G1 to G7), almost no discrimination errors occurred as well in the discrimination tasks of textures rendered by the Piezotact device. On the contrary, the average FIV RMS amplitudes for samples G8 and G9 resulted to be equal (Fig. 11). The FIV RMS was very similar for samples from G10 to G13. This agrees as well with the measured roughness scale, as shown in Table 1, since samples from G10 to G13 have very close S_a. These samples (from G8 to G13) have often been confused in all discrimination tasks. Specifically, in task 1 concerning real textures, all discrepancies between the roughness judgement by the participants and the order of the glasspapers concern textures from G8 to G13 (set 05 and set 06).

A more in-depth analysis was conducted by comparing, for each set of samples, the FIV RMS amplitudes for each of the 10 volunteers. The textures that were never confused with the discrimination of real textures (task 1) show well-defined trends and well different FIV RMSs for almost all participants: An example (set 03) is shown in Fig. 12(a). On the contrary, in task 1, all the discrimination errors concerned sets 05 and 06, in

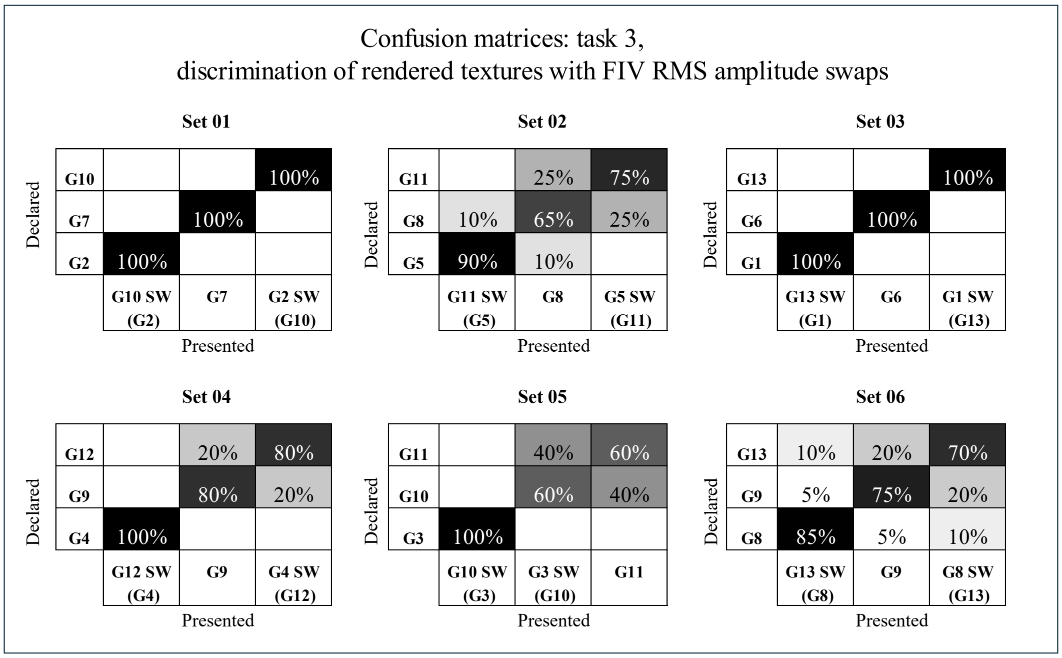

Fig. 10 Results of discrimination campaign of rendered textures with the Piezotact device with FIV RMS amplitude swaps of pairs of samples (task 3).

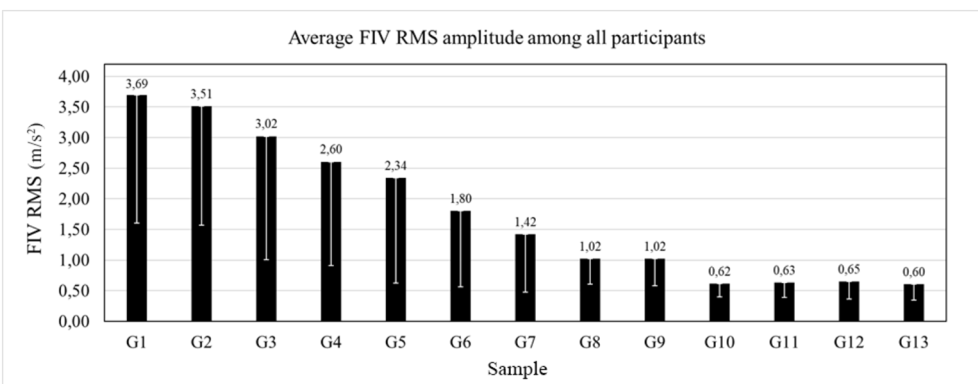

Fig. 11 FIV RMS amplitude by active touch of the 13 isotropic textures. For each texture, an average RMS amplitude among all the participant's FIV (10 strokes for each participant) is shown.

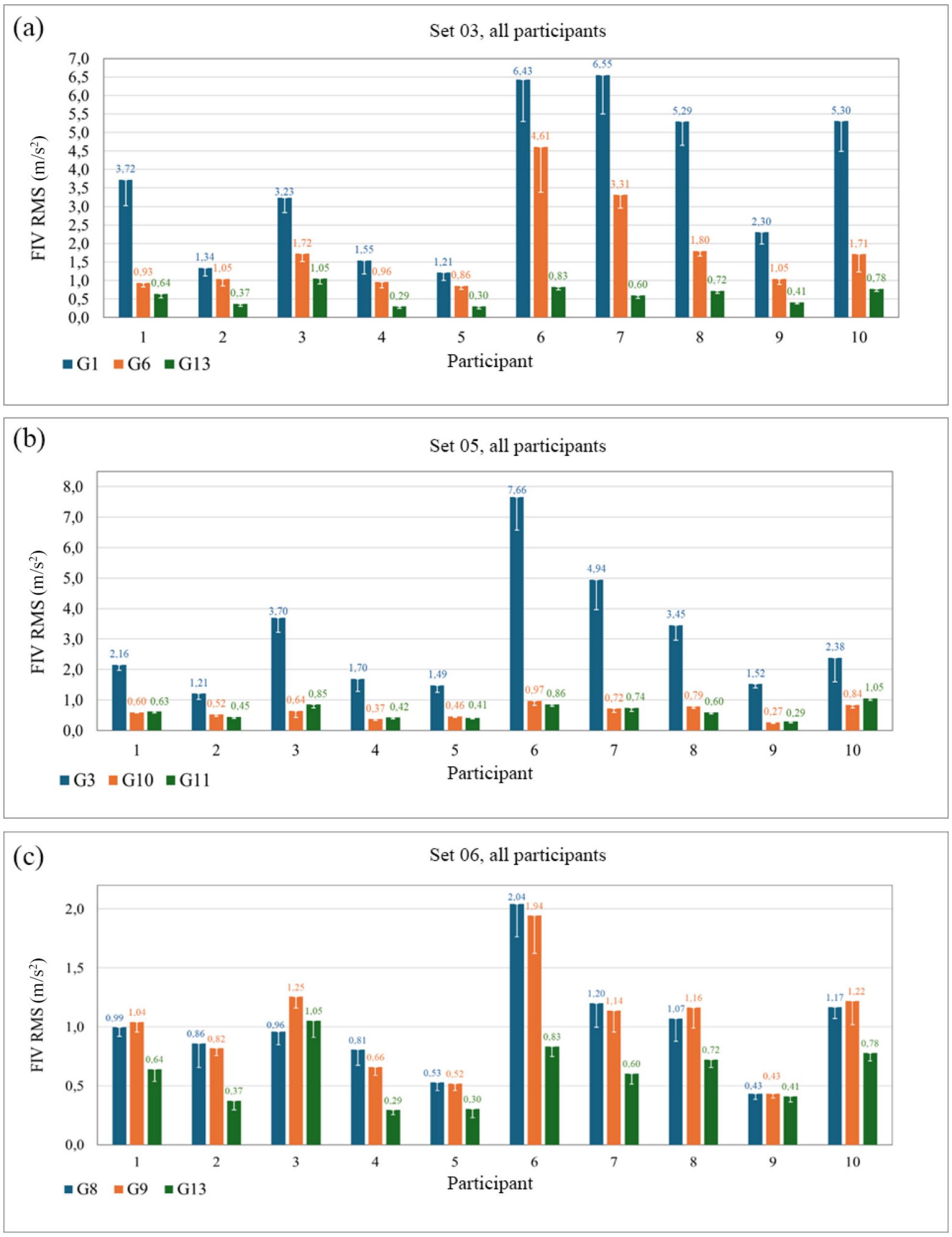

Fig. 12 FIV RMS amplitudes for all 10 participants for surface samples belonging to set 03, set 05, and set 06 (the *y*-scales in (a), (b), and (c) are different for readability of the graphs).

agreement with the FIV RMS amplitudes shown in Figs. 12(b) and 12(c). In particular, in set 05, the G3 sample was always sorted as the roughest by all participants, while the G10 and G11 samples had a 70% classification of the G11 as rougher than the G10; this is reflected by FIV, whereby the G10 and G11 samples have very close RMS amplitudes for all participants, well different from G3, as it can be seen in Fig. 12(b). In set 06, several inversions occurred in the discrimination of real surfaces. For almost all participants, the FIV associated with the G8 and G9 samples are very close, while the G13 sample generally has a slightly lower amplitude, but the trend is not entirely uniform among the participants. In general, from the analysis of the 3 discrimination tasks, starting from sample G8 to G13 there is a non-uniformity in the discrimination and in the roughness clustering between the participants (Figs. 8–10); Fig. 12 confirms that no well-defined trends can be observed when the FIV of different samples present similar amplitudes.

Figure 13 shows the PSD of the measured FIV, which was then rendered by the Piezotact device in order to perform tasks 2 and 3, for 2 different volunteers who took part in the sensory campaign, taken as an example. Overall, for the different volunteers, by comparing the FIV associated with the different surface samples, it is possible to highlight that the FIV show a similar frequency distribution, while the characteristic that varies most from one surface sample to another is the amplitude of the vibrations. In general, the amplitude of the vibrations decreases as the roughness of the samples decreases. This observation confirms that the key parameter for the differentiation of isotropic textures is the FIV amplitude rather than their frequency distribution.

When considering differences between subjects, although the vibrations qualitatively present the same trend for different volunteers, they have very different amplitudes from one subject to another. This can be due to the different sliding speeds adopted by the participants to actively scan the textures, the different characteristics of the participants' fingers (moisture, skin elasticity, sebum formation, fingerprint characteristics, etc.), the small variations in the contact boundary conditions such as finger/surface inclination and contact force, etc.

Figure 14 shows the PSD of the FIV measured for the smoothest samples, G8, G9, G10, G11, G12, G13, for 2 different volunteers. The spectra, for these samples, and even more particularly for samples from G10 to G13, are very similar, both in terms of amplitude and frequency distribution. It is no longer possible to appreciate a trend of decreasing vibration amplitudes, with respect to the glasspaper grit rating, in agreement with the RMS analysis in Figs. 11 and 12. This contributes to explaining the errors and difficulties occurred in the discrimination of the smoothest samples (from G8 to G13) in all the discrimination tasks.

A more in-depth analysis has been carried out on the spectra of vibrations replicated by Piezotact for individual volunteers. In particular, in the discrimination of rendered textures (tasks 2 and 3) the presence of some discrimination errors that were not present in the discrimination of real textures has been observed, which affected sets 02 and 04. By analyzing the specific spectra of the volunteers, it is possible to explain the greatest part of the errors that occurred in sets 02 and 04 by means of the FIV spectra. In particular, some volunteers committed discrimination errors in task 3, concerning the discrimination of rendered textures with swaps of FIV amplitudes for pairs of samples, while they correctly discriminated the same pairs of samples in task 2 (without FIV amplitude swaps). It is found that, for these volunteers, the process of swapping of the amplitudes of FIV, based on the sole RMS, led to some spectral modifications that explained the discrimination errors in task 3. An illustration is given in Fig. 15. Set 04 is composed by samples G4, G9 and G12, to perform task 2, and by samples G4 SW (with G12), G8 and G12 SW (with G4), to perform task 3. Figure 15(a) depicts all the 5 spectra obtained when rendering the set 04, for the volunteer taken as an example. Figure 15(b) shows the comparison between the PSD spectra of G8 and G12, used to perform task 2, showing higher amplitude components for almost all the spectra for G8, compared to G12; consistently, the volunteer correctly discriminated such samples in task 2. Figure 15(c) illustrates the spectra G8 and G4 SW (G12), where G4 SW (G12) has the frequency spectral distribution of sample G4 but the FIV RMS amplitude of G12. G4 SW shows significantly larger low-frequency components than G8, which explains why the volunteer swapped the two associated textures in task 3. Although the RMS amplitude is equal for G12 and G4 SW, their frequency distribution is definitely different, and this has played a role in the discrimination of the rendered textures. It should be kept in mind that tactile perception is a result of the simultaneous sensation and elaboration of several stimuli, including several features that are more or less related to the surface features. The results presented in this work support the hypothesis that the parameter that most affects the differentiation and discrimination of the isotropic textures, tested in this work, is the average amplitude of FIV. However, the presented analysis shows that the frequency distribution of the FIV plays a role as well in the discrimination, especially for fine textures. Moreover, fine and coarse textures can be related to different perception mechanisms [33], and different mechanoreceptors bring

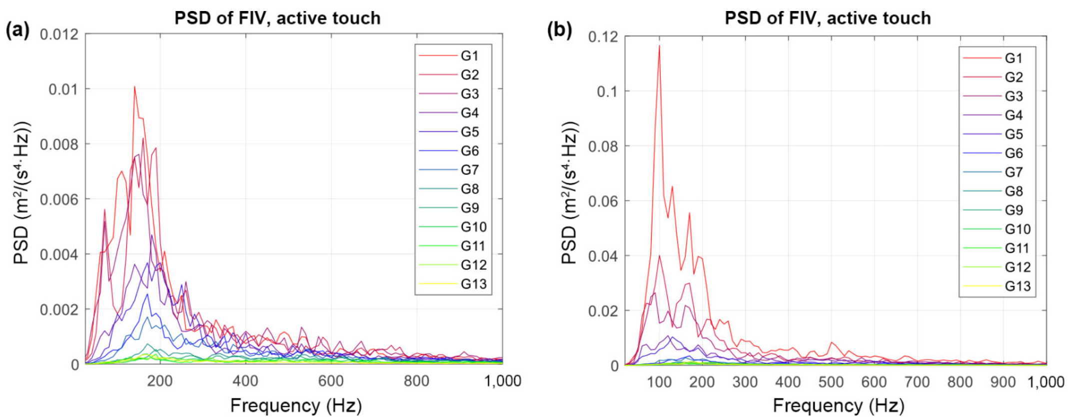

Fig. 13 PSDs of FIV measured by the active scanning of the 13 isotropic textures, and then rendered by the Piezotact, for 2 different volunteers (the *y*-scales in (a) and (b) are different for readability of the plots).

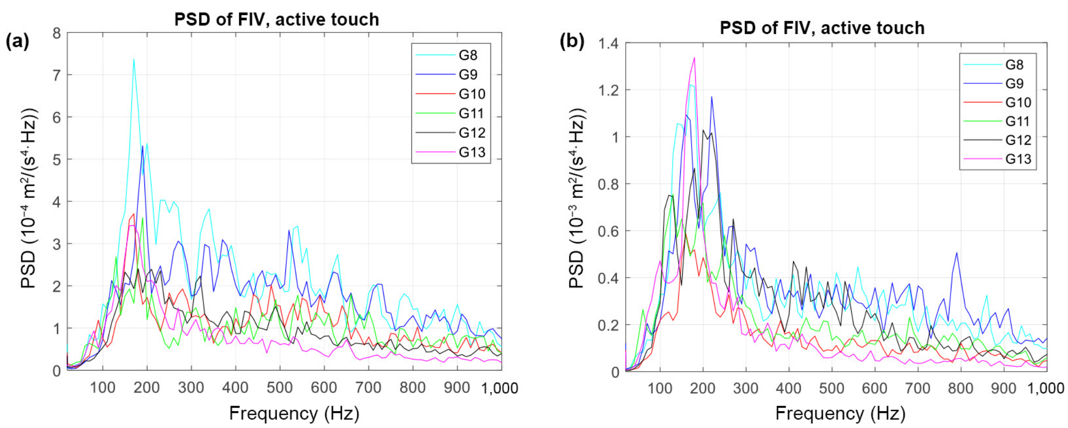

Fig. 14 PSDs of FIV for 2 different volunteers, associated with active scanning of smoother samples G8, G9, G10, G11, G12, G13 (the *y*-scales in (a) and (b) are different for readability of the plots).

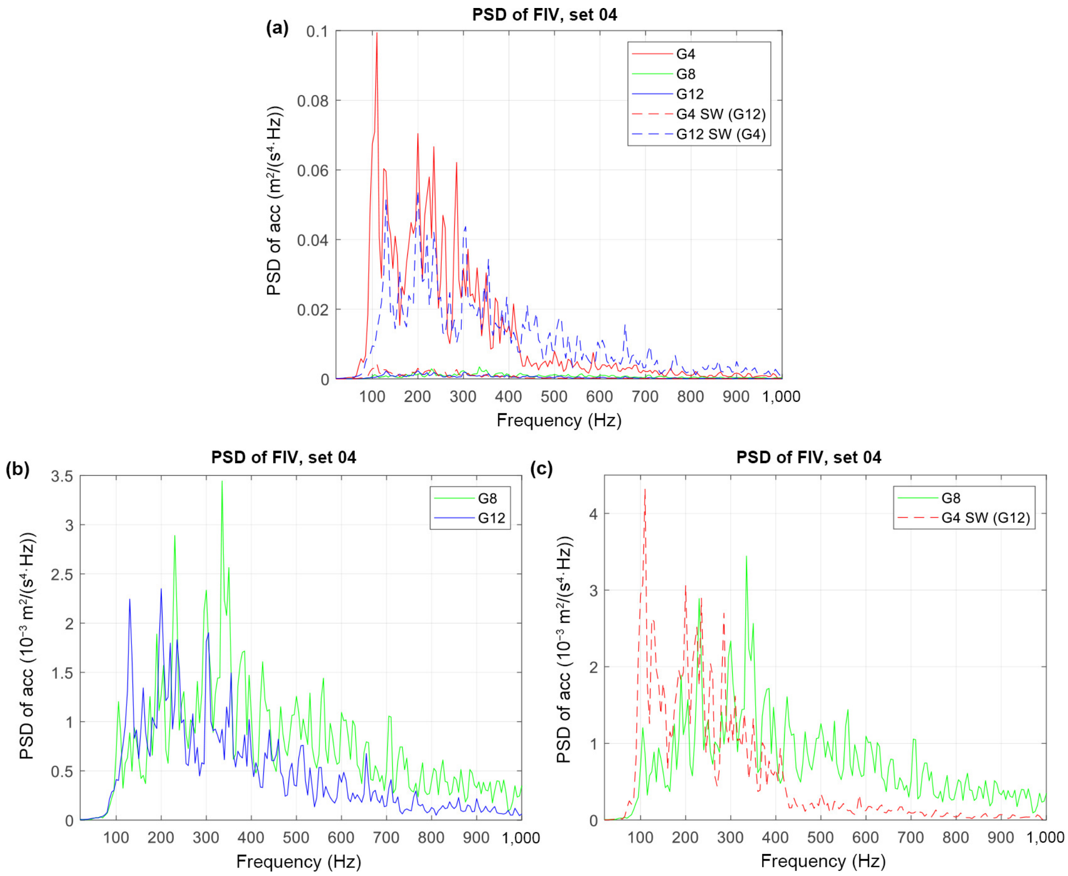

Fig. 15 PSD spectra of FIV obtained for rendering to perform tasks 2 and 3 for the textures in set 04 for a participant who correctly discriminated in task 2 but not in task 3: (a) all the spectra, (b) spectra of G8 and G11, (c) spectra of G8 and G4 SW with G11.

information on both spatial and temporal codes [9]. Nevertheless, the overall results, found with the specific set of tested topographies having similar spectrum distribution, corroborate the role of the FIV amplitude as well. The FIV features have been modulated here to modify the texture perception, by modifying the main driving parameters for their discrimination.

4 Conclusions

In the present work, a vibrotactile rendering device has been used to mimic tactile stimuli for perception of isotropic textures and to mislead texture perception by manipulating the simulated stimuli. FIV have been measured during the exploration of the isotropic sample textures and rendered using the Piezotact device. A sensory campaign has been carried out on 10 volunteers, which involved a task of discrimination of real textures and two tasks of discrimination of textures rendered by Piezotact, replicating only the FIV stimuli. A first task of discrimination of rendered textures has been carried out by replicating the FIV measured during the exploration of the textures. The second task of discrimination of rendered textures has been carried out with "fake" textures obtained by manipulating the measured FIV, where the RMS amplitudes of the FIV have been swapped for some pairs of samples. The results showed that by swapping the amplitude of the FIV stimuli the volunteers were misled and were induced to discriminate the textures consistently with the FIV amplitude. The results of the sensory campaign have been then analyzed and interpreted in correlation with the FIV, which allowed us to explain almost all the results of the discrimination of both real and simulated textures. Samples that have been often confused by volunteers had very close FIV RMS amplitudes, while samples that have been correctly discriminated had definitely different induced vibration amplitudes.

It should be kept in mind that, for the present analysis, isotropic surfaces with similar large band spectrum distributions have been used. This specific feature allows for highlighting the role of the FIV amplitude when interacting with such isotropic surfaces. In a previous work [38], surfaces with periodical textures were tested, highlighting a dominant role of the frequency distribution. It is expected that, when exploring natural surfaces with more complex spectral distribution, as reported in Refs. [8, 54], both the parameters play a role in the discrimination process.

In addition, the results of the discrimination campaign of rendered textures, with and without FIV RMS swaps, have been explained by means of FIV spectra, corroborating the predominant role of FIV amplitude, but also highlighting a role of spectral distribution, albeit less preponderant for the tested surfaces. This has been possible thanks to the innovative approach of using the tactile devices to replicate the vibrations measured by the exploration of the textures and to appropriately alter their amplitude and frequency distribution features, in order to create new, virtually perceived textures.

Acknowledgements

The authors thank Antoine Latour from CEA LITEN and ARKEMA-Piezotech for providing the used electro-active polymer piezoelectric actuators for this study.

Funding

This work was supported by the project EMOTACT (ANR-24-

CE28-0649-03), funded by the French "Agence Nationale de la Recherche" (ANR), and by the Sapienza University of Rome.

Compliance with ethical standards

All participants involved in the experimentation gave their written informed consent to take part in this study, which conformed to the ethical standards set out in the Declaration of Helsinki. The experimentation was approved by the research ethics committee CERSTAPS (IRB00012476-2021-09-12-140).

Declaration of competing interest

The authors have no competing interests to declare that are relevant to the content of this article.

Availability of data and materials

The data that support the findings of this study are available from the corresponding author upon reasonable request.

Author contributions

Livia Felicetti: conceptualization, data curation, formal analysis, investigation, methodology, validation, project administration, writing original draft, review and editing. Erich Chatelet: conceptualization, funding acquisition, resources, methodology, project administration, supervision, writing review and editing. Francesco Massi: conceptualization, funding acquisition, resources, methodology, project administration, supervision, writing review and editing.

References

[1] Johnson K. The roles and functions of cutaneous mechanoreceptors. *Curr Opin Neurobiol* **11**(4): 455–461 (2001)
[2] Costes A, Danieau F, Argelaguet F, Guillotel P, Lecuyer A. Towards haptic images: A survey on touchscreen-based surface haptics. *IEEE Trans Haptics* **13**(3): 530–541 (2020)
[3] Basdogan C, Giraud F, Levesque V, Choi S. A review of surface haptics: Enabling tactile effects on touch surfaces. *IEEE Trans Haptics* **13**(3): 450–470 (2020)
[4] Choi S, Kuchenbecker K J. Vibrotactile display: Perception, technology, and applications. *Proc IEEE* **101**(9): 2093–2104 (2013)
[5] Gueorguiev D, Vezzoli E, Mouraux A, Lemaire-Semail B, Thonnard J L. The tactile perception of transient changes in friction. *J R Soc Interface* **14**(137): 20170641 (2017)
[6] Torres D A, Kaci A, Giraud F, Giraud-Audine C, Amberg M, Clenet S, Lemaire-Semail B. PCA model of fundamental acoustic finger force for out-of-plane ultrasonic vibration and its correlation with friction reduction. *IEEE Trans Haptics* **14**(3): 551–563 (2021)
[7] Tang W, Zhang S, Yu C, Zhu H, Chen S, Peng Y. Tactile perception of textile fabrics based on friction and brain activation. *Friction* **11**(7): 1320–1333 (2023)
[8] Manfredi L R, Saal H P, Brown K J, Zielinski M C, Dammann J F III, Polashock V S, Bensmaia S J. Natural scenes in tactile texture. *J Neurophysiol* **111**(9): 1792–1802 (2014)
[9] Weber A I, Saal H P, Lieber J D, Cheng J W, Manfredi L R, Dammann J F III, Bensmaia S J. Spatial and temporal codes mediate the tactile perception of natural textures. *P Natl Acad Sci USA* **110**(42): 17107–17112 (2013)
[10] Louyot E, Carpentier L, Chatelet E, Massi F, Cornuault P H. Influence of the finger inclination on its frictional interaction with micro-textured surfaces. *Tribol Int* **197**: 109815 (2024)
[11] Cornuault P H, Carpentier L, Bueno M A, Cote J M, Monteil G. Influence of physico-chemical, mechanical and morphological fingerpad properties on the frictional distinction of sticky/slippery surfaces. *J R Soc Interface* **12**(110): 20150495 (2015)
[12] Zhou X, Masen M A, Mo J, Shi X, He Y, Jin Z. Investigation of experimental devices for finger active and passive tactile friction analysis. *Chin J Mech Eng* **36**: 38 (2023)
[13] Sahli R, Prot A, Wang A, Müser M H, Piovarči M, Didyk P, Bennewitz R. Tactile perception of randomly rough surfaces. *Sci Rep* **10**: 15800 (2020)
[14] Chimata G P, Schwartz C J. Tactile discrimination of randomly textured surfaces: Effect of friction and surface parameters. *Biotribology* **11**: 102–109 (2017)
[15] Peyre K, Tourlonias M, Bueno M A, Spano F, Rossi R M. Tactile perception of textile surfaces from an artificial finger instrumented by a polymeric optical fibre. *Tribol Int* **130**: 155–169 (2019)
[16] Jiao J, Zhang Y R, Wang D X, Visell Y, Cao D K, Guo X W, Sun X Y. Data-driven rendering of fabric textures on electrostatic tactile displays. In: Proceedings of the IEEE Haptics Symposium, 2018: 169–174.
[17] Osgouei R H. Electrostatic friction displays to enhance touchscreen experience. In: *Modern Applications of Electrostatics and Dielectrics*. Xiao D M, Sankaran, Eds. London (UK): IntechOpen, 2020.
[18] Osgouei R H, Kim J R, Choi S. Data-driven texture modeling and rendering on electrovibration display. *IEEE Trans Haptics* **13**(2): 298–311 (2020)
[19] Cai S, Zhao L, Ban Y, Narumi T, Liu Y, Zhu K. GAN-based image-to-friction generation for tactile simulation of fabric material. *Comput Graph* **102**: 460–473 (2022)
[20] Wu S, Sun X, Wang Q, Chen J. Tactile modeling and rendering image-textures based on electrovibration. *Vis Comput* **33**(5): 637–646 (2017)
[21] Friesen R F, Klatzky R L, Peshkin M A, Colgate J E. Building a navigable fine texture design space. *IEEE Trans Haptics* **14**(4): 897–906 (2021)
[22] Grigorii R V, Klatzky R L, Colgate J E. Data-driven playback of natural tactile texture via broadband friction modulation. *IEEE Trans Haptics* **15**(2): 429–440 (2022)
[23] Wiertlewski M, Fenton Friesen R, Colgate J E. Partial squeeze film levitation modulates fingertip friction. *P Natl Acad Sci USA* **113**(33): 9210–9215 (2016)
[24] Watanabe T, Fukui S. A method for controlling tactile sensation of surface roughness using ultrasonic vibration. In: Proceedings of the IEEE International Conference on Robotics and Automation, 1995: 1134–1139.
[25] Camillieri B, Bueno M A, Fabre M, Juan B, Lemaire-Semail B, Mouchnino L. From finger friction and induced vibrations to brain activation: Tactile comparison between real and virtual textile fabrics. *Tribol Int* **126**: 283–296 (2018)
[26] Weiland B, Leclinche F, Kaci A, Camillieri B, Lemaire-Semail B, Bueno M A. Tactile simulation of textile fabrics: Design of simulation signals with regard to fingerprint. *Tribol Int* **191**: 109113 (2024)
[27] Heravi N, Culbertson H, Okamura A M, Bohg J. Development and evaluation of a learning-based model for real-time haptic texture rendering. *IEEE Trans Haptics* **17**(4): 705–716 (2024)
[28] Burns D A, Klatzky R L, Peshkin M A, Colgate J E. A low-parameter rendering algorithm for fine textures. *IEEE Trans Haptics* **15**(1): 57–61 (2022)
[29] Burns D A, Klatzky R L, Peshkin M A, Colgate J E. The Single-Pitch Texel: A flexible and practical texture-rendering algorithm. *PNAS Nexus* **3**: pgad452 (2023)
[30] Snyder O, Almasi R, Fang C, Klatzky R L, Stetten G. Assessment of surface rendering with 1 DoF vibration. *Comput Meth Biomech Biomed Eng Imag Vis* **9**(4): 400–406 (2021)
[31] Alma U A, Rosenkranz R, Altinsoy M E. Perceptual substitution based haptic texture rendering for narrow-band reproduction. *IEEE Trans Haptics* **16**(2): 204–214 (2023)
[32] Liu Z, Kim J T, Rogers J A, Klatzky R L, Colgate J E. Realism of tactile texture playback: A combination of stretch and vibration. *IEEE Trans Haptics* **17**(3): 441–450 (2024)
[33] Hollins M, Risner S R. Evidence for the duplex theory of tactile texture perception. *Percept Psychophys* **62**(4): 695–705 (2000)
[34] BensmaÏa S J, Hollins M. The vibrations of texture. *Somatosens Mot Res* **20**(1): 33–43 (2003)
[35] Shin S, Osgouei R H, Kim K D, Choi S. Data-driven modeling of

isotropic haptic textures using frequency-decomposed neural networks. In: Proceedings of the IEEE World Haptics Conference, 2015: 131–138.
[36] Strohmeier P, Hornbæk K. Generating haptic textures with a vibrotactile actuator. In: Proceedings of the CHI Conference on Human Factors in Computing Systems, 2017: 4994–5005.
[37] Culbertson H, Unwin J, Kuchenbecker K J. Modeling and rendering realistic textures from unconstrained tool-surface interactions. *IEEE Trans Haptics* **7**(3): 381–393 (2014)
[38] Felicetti L, Chatelet E, Latour A, Cornuault P H, Massi F. Tactile rendering of textures by an electro-active polymer piezoelectric device: Mimicking friction-induced vibrations. *Biotribology* **31**: 100211 (2022)
[39] Felicetti L, Chatelet E, Massi F. Dynamic analysis of a tactile device for mimicking mechanical stimuli responsible for texture perception. In: *Special Topics in Structural Dynamics & Experimental Techniques*. New York (USA): River Publishers, 2025: 141–145.
[40] Liu G, Zhang C, Sun X. Tri-modal tactile display and its application into tactile perception of visualized surfaces. *IEEE Trans Haptics* **13**(4): 733–744 (2020)
[41] Mouchnino L, Camillieri B, Faucheu J, Juganaru M, Moinon A, Blouin J, Bueno M A. Seeing the piles of the velvet bending under our finger sliding over a tactile stimulator improves the perception of the fabric. *J R Soc Interface* **21**(220): 20240368 (2024)
[42] Culbertson H, Kuchenbecker K J. Importance of matching physical friction, hardness, and texture in creating realistic haptic virtual surfaces. *IEEE Trans Haptics* **10**(1): 63–74 (2017)
[43] Shin S, Choi S. Effects of haptic texture rendering modalities on realism. In: Proceedings of the 24th ACM Symposium on Virtual Reality Software and Technology, 2018: 1–5.
[44] Kong K, Wang L, Wu H, Le Z, Zhang Y, Wang Z, Yu Z, Wu X, Li L, Li W, et al. Skin-inspired multimodal tactile sensor aiming at smart space extravehicular multi-finger operations. *Chem Eng J* **498**: 154870 (2024)
[45] Massimiani V, Weiland B, Chatelet E, Cornuault P H, Faucheu J, Massi F. The role of mechanical stimuli on hedonistic and topographical discrimination of textures. *Tribol Int* **143**: 106082 (2020)
[46] Di Bartolomeo M, Morelli F, Tonazzi D, Massi F, Berthier Y. Investigation of the role of contact-induced vibrations in tactile discrimination of textures. *Mech Ind* **18**(4): 404 (2017)
[47] Faucheu J, Weiland B, Juganaru-Mathieu M, Witt A, Cornuault P H. Tactile aesthetics: Textures that we like or hate to touch. *Acta Psychol* **201**: 102950 (2019)
[48] Cesini I, Ndengue J D, Chatelet E, Faucheu J, Massi F. Correlation between friction-induced vibrations and tactile perception during exploration tasks of isotropic and periodic textures. *Tribol Int* **120**: 330–339 (2018)
[49] Felicetti L, Sutter C, Chatelet E, Latour A, Mouchnino L, Massi F. Tactile discrimination of real and simulated isotropic textures by Friction-Induced Vibrations. *Tribol Int* **184**: 108443 (2023)
[50] Felicetti L, Chatelet E, Bou-Saïd B, Latour A, Massi F. Investigation on the role of the finger Transfer Function in tactile rendering by friction-induced-vibrations. *Tribol Int* **190**: 109018 (2023)
[51] Felicetti L, Chatelet E, Latour A, Massi F. Analysis and mimicking of contact vibrations, induced by touching isotropic surface textures. In: Proceedings of the International Conference on Noise and Vibration Engineering, 2022: 810–821.
[52] Zhou X, Mo J L, Li Y Y, Xiang Z Y, Yang D, Masen M A, Jin Z M. Effect of finger sliding direction on tactile perception, friction and dynamics. *Tribol Lett* **68**(3): 85 (2020)
[53] Natsume M, Tanaka Y, Kappers A M L. Individual differences in cognitive processing for roughness rating of fine and coarse textures. *PLoS One* **14**(1): e0211407 (2019)
[54] Dacleu Ndengue J, Cesini I, Faucheu J, Chatelet E, Zahouani H, Delafosse D, Massi F. Tactile perception and friction-induced vibrations: Discrimination of similarly patterned wood-like surfaces. *IEEE Trans Haptics* **10**(3): 409–417 (2017)
[55] Hu J, Zhang X, Yang X, Jiang R, Ding X, Wang R. Analysis of fingertip/fabric friction-induced vibration signals toward vibrotactile rendering. *J Text Inst* **107**: 967–975 (2016)
[56] Jiang R, Hu J, Yang X, Ding X. Analysis of fingertip/textile friction-induced vibration by time-frequency method. *Fibers Polym* **17**(4): 630–636 (2016)
[57] Fagiani R, Massi F, Chatelet E, Costes J P, Berthier Y. Contact of a finger on rigid surfaces and textiles: Friction coefficient and induced vibrations. *Tribol Lett* **48**(2): 145–158 (2012)
[58] Koç İ M, Aksu C. Tactile sensing of constructional differences in fabrics with a polymeric finger tip. *Tribol Int* **59**: 339–349 (2013)
[59] Greenspon C M, McLellan K R, Lieber J D, Bensmaia S J. Effect of scanning speed on texture-elicited vibrations. *J R Soc Interface* **17**(167): 20190892 (2020)
[60] Ding S, Pan Y, Zhao X. Humanoid identification of fabric material properties by vibration spectrum analysis. *Sensors* **18**(6): 1820 (2018)
[61] Lacerra G, Di Bartolomeo M, Milana S, Baillet L, Chatelet E, Massi F. Validation of a new frictional law for simulating friction-induced vibrations of rough surfaces. *Tribol Int* **121**: 468–480 (2018)
[62] Li Y, Zhou X, Bai P, Xiang Z, Meng Y, Ma L, Tian Y. Experiment and modelling of texture and sliding direction dependence on finger friction behavior. *Friction* **12**(9): 1955–1968 (2024)
[63] Zhou X, Mo J L, Li Y Y, Xu J Y, Zhang X, Cai S, Jin Z M. Correlation between tactile perception and tribological and dynamical properties for human finger under different sliding speeds. *Tribol Int* **123**: 286–295 (2018)
[64] Camillieri B, Bueno M A. Influence of finger movement direction and fingerprints orientation on friction and induced vibrations with textile fabrics. *Tribol Lett* **69**(4): 143 (2021)
[65] Prevost A, Scheibert J, Debrégeas G. Effect of fingerprints orientation on skin vibrations during tactile exploration of textured surfaces. *Commun Integr Biol* **2**(5): 422–424 (2009)
[66] Natsume M, Tanaka Y, Sano A. Skin-propagated vibration for roughness and textures. In: Proceedings of the World Automation Congress, 2016: 1–6
[67] Godard N, Allirol L, Latour A, Glinsek S, Gérard M, Polesel J, Domingues Dos Santos F, Defay E. 1-mW vibration energy harvester based on a cantilever with printed polymer multilayers. *Cell Rep Phys Sci* **1**(6): 100068 (2020)

Livia Felicetti is currently a researcher at the Department of mechanical and Aerospace Engineering of the Sapienza University of Rome, Italy. She received her joint Ph.D. degree in theoretical and applied mechanics at the Sapienza University of Rome, Italy, and in mechanical engineering at the National Institute of Applied Sciences (INSA) of Lyon, France, in 2024. Her research interests are in the field of applied mechanics, tribology, and biomechanics, with a particular focus on tactile perception.

Eric Chatelet received his Ph.D. degree in mechanical engineering from the Franche-Comté University (Besancon, France) in 1994. Since 1997, he is an assistant professor in the Department of Mechanical Engineering, INSA Lyon, France. His research interests (in the Laboratory of Mechanics of Contacts and Structures (LaMCoS, UMR CNRS 5259, INSA Lyon)) include the vibrations and dynamics of structures. They focus on the testing of on-board (rotating or not) systems (see Equipex PHARE) as well as the dynamics of contacts (friction induced vibrations) with many applications such as energy transfer or tactile perception.

Francesco Massi, professor, received his Ph.D. degree in "theoretical and applied mechanics" at the University of Rome "La Sapienza" and the Ph.D. degree in "mechanical engineering" at the INSA of Lyon in 2006. In 2003 he received his degree in mechanical engineering from La Sapienza, following a training period at the Carnegie Mellon University in Pittsburgh (USA). Between 2007 and 2012 he held the position of "Maître de conferences" at the Contact and Structural Mechanics Laboratory of the INSA of Lyon. He joined as visiting scholar the Tribology Research Institute of Southwest Jiaotong University, Chengdu, China (August 2019) and the Laboratoire de Neurosciences Cognitives at the Aix Marseille Université, France (June 2022) and the LamCube laboratory at the university Central Lille, France (June 2025). He is currently full professor of applied mechanics at the Department of Mechanical and Aerospace Engineering at the University of Rome "La Sapienza". As a member of the Steering Committee of the Italian Association of Tribology, he is actively involved in conference committees, journal editorial boards and heading projects aimed at the dissemination of tribology in academia and its technological transfer in industry. His main research interest lies in tribology, dynamics and biomechanics. Currently, his activities focus on contact instabilities, contact interface dynamics, friction-induced vibrations, tactile perception, and greased contacts.